FISEVIER

Contents lists available at ScienceDirect

International Journal of Pharmaceutics

journal homepage: www.elsevier.com/locate/ijpharm



Preparation of multifunctional Janus nanoparticles on the basis of SPIONs as targeted drug delivery system



Behrad Shaghaghi^a, Sepideh Khoee^{a,*}, Shahin Bonakdar^b

- ^a Polymer Laboratory, School of Chemistry, College of Science, University of Tehran, PO Box 14155 6455, Tehran, Iran
- ^b National Cell Bank of Iran, Pasteur Institute of Iran, Tehran, Iran

ARTICLE INFO

Keywords:
Drug delivery
Nanomedicine
Janus nanoparticle
Targeted delivery
Superparamagnetic iron oxide nanoparticles
(SPIONs)
Blood-brain barrier (BBB)

ABSTRACT

Passing the Blood-Brain-Barrier (BBB) is a challenging aspect in nanomedicine. Utilizing surfactant particles is reported to be a potent strategy for easier BBB penetration. On the other hand, loading different functional molecules on a single particle is therapeutically and economically beneficial. In this study, multifunctional amphiphilic Janus nanoparticles have been prepared on the basis of superparamagnetic iron oxide nanoparticles. This Janus platform is armed with folic acid targeting agent and Doxorubicin (DOX) drug that have been conjugated on different sides of the nanoparticles. DOX has been conjugated via imine bond that makes these particles pH sensitive. Chemo-physical characters, in-vitro drug release pattern and toxicity of nanoparticles on rat C6 glioma cell line were studied that confirmed the preparation and pH-dependent behavior of nanoparticles. Microscopy observations showed the Janus morphology of nanoparticles and their cell penetration behavior. Prepared Janus nanoparticle can be utilized as a multifunctional nanomedicine platform for brain cancer treatment.

1. Introduction

Glioblastoma multiforme (GBM) may be the deadliest and most frequent malignant primary brain tumor with a median survival of about 14.6 months (Thomas et al., 2017) and a five-year survival rate of about 5.1% (Sun et al., 2017). A combined modality therapy of chemotherapy, radiation, and surgery is the standard treatment for glioblastoma (Lallana and Abrey, 2003) which unfortunately leads to the death of 80% of patients (Quirk et al., 2015). Since malignant tumor cells migrate to normal brain tissues, they would be left behind after tumor resection, causing tumor recovery (Munthe et al., 2016). Superparamagnetic iron oxide nanoparticles (SPIONs) are the most popular magnetic nanoparticles (MNPs). SPION-dextran-based MRI contrast agent has been approved by the FDA for human clinical approaches. It can also be used as a heat-generating agent for hyperthermia-based therapy (Stone et al., 2011) and an efficient magnetic force-guided drug delivery vehicle (Lee et al., 2015; Mahmoudi et al., 2010). Surface modification is necessary to avoid the rapid clearance of bare MNPs from blood circulation. It must be as trustworthy as the "Trojan horse" to remain in the circulation, reach the target tissue via passive or active targeting, and release the therapeutic ligand (Basiruddin et al., 2010). Polyethylene glycol (PEG) is one of the best, most flexible, and highly hydrophilic coating biocompatible polymers

that reduce the MNPs uptake by macrophages (Zhang et al., 2002) and increase the blood circulation time. Despite its benefits, the cell uptake of PEG-coated MNPs is not appreciable. Thus, there have to be other complementary strategies to solve this problem (Li et al., 2013). Conjugating folic acid (FA) on PEG can improve the tumor accumulation of nanoparticles (NPs) and intracellular delivery (Hayashi et al., 2013). To use NPs as drug delivery systems, the preferable drug must be either conjugated on the particle or simply be loaded between polymer chains. Different drugs such as temozolomide and doxorubicin (DOX) have been used as the first-line treatment or combination therapy agents along with radiotherapy or surgery, for patients with glioma (Ellor et al., 2014). Ninety-eight percent of candidate chemotherapeutic drugs are not able to traverse the blood-brain barrier (BBB) and the blood-brain tumor barrier (BBTB). On the other hand, hydrophobic drugs such as DOX that can more easily pass through this obstacle are not appropriate for IV injection (Gao et al., 2017). Even if these cytotoxic drugs are able to pass BBB, they may not achieve the proper therapeutic dose in cancerous cells. Increasing the drug dose may seem to solve the problem but it increases the drug's side-effects and would affect the patients' quality of life during treatment (Sun et al., 2017). The short blood circulation time is another shortcoming of anticancer drugs that affects the drug dose and dosing intervals. Many strategies have been proposed to overcome these problems by designing effective drug

E-mail address: khoee@khayam.ut.ac.ir (S. Khoee).

^{*} Corresponding author.

delivery systems which are able to transport and safeguard hydrophobic drugs, alter the macrophage uptake to prolong circulation time, lower the drug dose to decrease side-effects, and penetrate BBB. From among these strategies, the use of NPs to carry drugs through BBB seems to be an appropriate methodology because they can be tailored to be small enough to pass blood barriers, non-toxic, biocompatible, biodegradable, stable in blood, non-inflammatory, scalable, cost-effective, and able to transport different types of molecules (Lockman et al., 2002). Since the first time hexapeptide dalargin was delivered to the brain using NPs (Kreuter, 2001), NPs have been widely used in researches related to the central nervous system (CNS) drug delivery agents because of their beneficial characters (Kang et al., 2018). In the case of active brain drug delivery, it has been reported that the application of surfactant systems can play a significant role in delivering molecules through BBB (Neves et al., 2017).

Polysorbate, a polyoxyethylene-based amphiphilic surfactant, has been utilized in different NPs for brain drug delivery. Since medicinecontaining polysorbates have shown pseudoallergies in some cases, polyoxyethylene sorbitol oleate was used as a safe alternative (Sun et al., 2017). Amphiphilic Janus NPs have anisotropic physical and/or chemical properties and can express a surfactant behavior. Most important features determining Janus particles' functionality are their amphiphilicity, size, shape, and surface active agents. Spherical Janus particles have three-time greater adsorption energy and much higher surface activity compared to homogeneous surfactants (Tu and Lee, 2014) and, as a drug delivery system, Janus NPs have the best cell uptake efficiency compared to other dual ligand targeting system (Xia et al., 2017). These particles can be decorated to have extremely different sides which can be individually designed to exhibit distinct functionalities in a single particle (Sundararajan et al., 2018). Using these particles, it is possible to make multifunction nanomedicines which have various functional ligands with different chemical and physical properties, used for targeting, diagnosis, and therapy.

Here, we prepared SPION-based multifunctional Janus NPs designed to pass through the BBB to accumulate in tumor via the FA ligand and deliver doxorubicin in the acidic stimuli of malignant glioma cells. The characteristics of prepared NPs were investigated by proton nuclear magnetic resonance (1H NMR), Fourier-transform infrared (FT-IR), vibrating-sample magnetometer (VSM), transmission electron microscopy (TEM), thermo-gravimetric analysis (TGA), and dynamic laser light scattering (DLS). The drug release pattern of the drug-conjugated Janus NP (DOX-PCL-SPION-sPEG-FA) was measured in vitro, and in vitro bio-interaction tests have been reported.

2. Materials and methods

The materials we used in this work included FeCl2·.4H2O, FeCl3:6H2O, paraffin wax granules, (3-aminopropyl)triethoxysilane (APTES), (3-mercaptopropyl) triethoxysilane (MPTES), folic acid (FA), polyoxyethylene (20) sorbitan monooleate, di-tert-butyl dicarbonate (BOC), propargyl alcohol, tin(II) 2-ethylhexanoate, ε-caprolactone, N,N-dicyclohexylcarbodiimide (DCC), 4-dimethylaminopyridine (DMAP), sodium azide (NaN3), copper bromide (CuBr) and N,N,N',N",N"-pentamethyl diethylenetriamine (PMDETA) were obtained from Sigma-Aldrich. E-Caprolactone, dichloromethane (DCM), N, N-dimethylformamide (DMF), hydrochloric acid (HCl), epichlorohydrin, stannous octoate (Sn(Oct)2), 4-Toluenesulfonyl chloride (TsCl), N-hydroxysuccinimide (NHS) were all purchased from Merck Chemical Co. Triethylamine (TEA) was obtained from Fluka. Doxorubicin hydrochloride solution (2 mg/ml) was purchased from Pfizer. All reagents and solvents were of analytical grade and used without any purification.

2.1. Drug conjugated Janus nanoparticle synthesis

Synthesis of drug-conjugated Janus NPs (DOX-PCL-SPION-sPEG-FA)

was performed in four main steps: preparing core particle, hydrophilic part synthesis, hydrophobic part synthesis, and Janus NPs combination.

2.1.1. Preparation of core particle

2.1.1.1. Synthesis of magnetite Fe3O4 nanoparticles. The chemical coprecipitation method was employed to prepare Fe3O4 NPs in an aqueous solution. The alkaline precipitation of FeCl3 and FeCl $_2$ would yield superparamagnetic iron oxide NPs (SPION). FeCl $_2$ ·4H $_2$ O (1 g) and FeCl $_3$ ·6H $_2$ O (2.6 g) were dissolved in 25 mL of deionized water at a 1:2 mol ratio in a three-necked round-bottom flask and degassed under an inert nitrogen atmosphere. Then, 10 mL of ammonia solution was added to the stirring mixture dropwise at 70 °C under nitrogen flow and stirred for 1 h using a mechanical stirrer to reach the desired size. The black mixture of magnetic NPs was magnetically separated and washed with deionized water (3 \times 25 mL) and ethanol (3 \times 20 mL).

2.1.1.2. Pickering emulsion. Janus SPIONs were prepared through the Pickering emulsion technique. Bare SPIONs were masked and immobilized in paraffin wax particles. Next, 1 g of SPION was dispersed in about 50 mL of distilled water for 20 min using an ultrasound sonicator. The mixture was poured into a cylindrical beaker and heated up to 75 °C while being stirred at 1900 rpm using a mechanical stirrer. Afterward, 10 g of paraffin wax granule was gradually added to the stirring mixture. Stirring was continued for another hour, and the amount of water and level of temperature were precisely controlled. The mixture was suddenly cooled down by pouring a large volume of freezing-cold distilled water into the mixture beaker to solidify wax particles and form an emulsion. The mixture was kept in the refrigerator for another hour to make the emulsion stable. Next, non-trapped and weakly trapped SPIONs were separated through decantation. As the SPION-stabilized colloidosomes float on the water, the non-attached SPIONs precipitated and could be collected from the mixture.

2.1.1.3. Grafting (3-mercaptopropyl) triethoxysilane on waxed SPIONs (SPION-SH). The unshielded side of waxed SPIONs was coated with MPTES (Khoee et al., 2015). SPION hydroxyl groups can react with MPTES in the presence of water. Thus, the half side of SPIONs was modified with the thiol functional group to be used in further thiol-ene click reaction. Five g of waxed SPIONs was dispersed in 40 mL of ethanol, containing 2 mL of MPTES and 1 mL of water. The mixture was let to stir overnight at 25 °C. Modified colloidosomes were then separated using an external magnetic field and washed with ethanol three times to remove unreacted MPTES. To release half-coated SPIONs from wax colloidosomes, the mixture was washed several times with hot chloroform and the particles were collected using a magnet.

2.1.1.4. Grafting azidated triethoxysilane on dewaxed SPIONs (N_3 -SPION-SH). The bare side of dewaxed SPION-SH was modified with azidated triethoxysilane. First, 1-azido-3-chloropropan-2-ol was synthesized from the reaction of sodium azide and epichlorohydrin as reported by Ryu et al. (Ryu et al., 2013). Then, 1-azido-3-chloropropan-2-ol was reacted with APTES to form azidated triethoxysilane. As the last step, azidated triethoxysilane was conjugated to the hydroxyl groups of dewaxed SPION-SH NPs. Briefly, a mixture of sodium azide (2 g, 0.031 mol), epichlorohydrin 0.031 mol), (2.86 g,tetrabutylammonium bromide (25 mg, 85 mmol) in water was let to stir overnight at 25 °C in a round-bottom flask covered by aluminum foil to prevent the photodegradation of azide groups. To purify the product, dichloromethane was added to the mixture and the organic nonaqueous layer was separated, dried over magnesium sulfate, and concentrated in a rotatory evaporator to yield azidated epichlorohydrin (1-azido-3-chloropropan-2-ol). Freshly prepared azidated epichlorohydrin (3.38 g, 25 mmol) was added to a stirring suspension of THF (10 mL) and potassium carbonate (6.9 g, 0.05 mol). APTES (5.85 mL, 0.025 mol) was gradually poured in the reaction

media at 25 °C. The mixture was refluxed at 65 °C for 18 h. The mixture was then filtered and concentrated to yield azidated triethoxysilane. As for the last step of grafting azidated triethoxysilane on dewaxed SPIONs, half-conjugated NPs (1 g, 0.344 mol silane) were dispersed in ethanol (40 mL) containing freshly prepared azidated triethoxysilane (0.344 mol) and H2O (1 mL). The mixture was let to stir overnight at 25 °C. Modified Janus NPs were then separated using an external magnetic field and washed in triplicate with ethanol to remove unreacted azidated triethoxysilane. All the noted steps were performed in a light-protected condition to prevent the photodegradation of azide functional groups. The Janus magnetic NP core was then conjugated with hydrophilic and hydrophobic polymers through click reactions.

2.1.2. Preparation of the hydrophilic side

The hydrophilic side of Janus NPs consists of acrylated star poly (ethylene glycol) that can be conjugated to the core NP via click reaction. In the last steps of preparing the final particle, folic acid is conjugated to the free terminal hydroxyl functional groups of star poly (ethylene glycol).

2.1.2.1. Star-shaped poly(ethylene glycol) preparation (sPEG). Star-shaped poly(ethylene glycol) can be obtained from polyoxyethylene (20) sorbitan monolaurate (tween 20) via saponification reaction as reported by Khoee et al. (Khoee et al., 2017a). Briefly, 10 mL (7.4 mmol) of polyoxyethylene (20) sorbitan monolaurate dissolved in 20 mL of THF and 1 g (17 mmol) of KOH was added to the solution in a round-bottom flask under reflux condition. After about 24 h, the produced mixture was added to hexane/acidic water (1:1) and separated via decantation. The aqueous phase, containing sPEG, was separated and neutralized and sPEG was extracted using dichloromethane. The purification process was repeated in triplicate, with the reaction yield of approximately 65%.

2.1.2.2. Mono(acryloyl)-functionalization of star poly (ethylene glycol) (Acl-sPEG). One of the four terminal hydroxyl functional groups of sPEG was acrylated through a previously reported procedure (Khoee et al., 2017a). Briefly, 2 mmol of sPEG (about 2.13 g) was dissolved in 25 mL of DCM, degassed with nitrogen flow in a three-necked round-bottom flask and cooled down to 0 °C. Next, 281 μ L (2 mmol) of triethylamine and 163 μ L (2 mmol) of acryloyl chloride were added. The solution was let to stir at 25 °C and nitrogen atmosphere for 24 h. To separate the triethylammonium hydrochloride salt, the resulting mixture was filtered and washed three times with 10 mL of aqueous sodium bicarbonate solution (10%) and three times with 10 mL of saturated aqueous sodium chloride solution. Acl-sPEG was extracted with DCM, dried over magnesium sulfate, filtered, and concentrated using a rotatory evaporator. The mono-acrylated sPEG reaction yield was about 75%.

2.1.3. Preparing the hydrophobic side

Propargyl alcohol was used as the initiator so that the prepared poly (\$\epsilon\$-caprolactone) (PCL) would have a free alkyne terminal group(-yne) for further click reaction with the azide groups of core NP. Briefly, 5 mL of \$\epsilon\$-caprolactone and 110 \$\mu\$L of propargyl alcohol were poured into a three-necked round-bottom flask and degassed with dried nitrogen. One drop of tin(II) 2-ethylhexanoate was added, the mixture was heated up to 110 °C, and stirring continued for 18 h. The mixture was cooled down to 25 °C and dissolved in a minimum amount of DMF. The produced OH-PCL-yne was precipitated in an excessive amount of cold water, separated, and dried. Reaction yield was approximately 84%.

2.1.3.1. Conjugating doxorubicin to OH-PCL-yne. Ethylenediamine was used as a proper crosslinker to conjugate DOX to the prepared yne-PCL-OH. PCL hydroxyl end group was first activated by tosyl chloride and then reacted with the free amine group of tert-butyloxycarbonyl (Boc)

protected ethylene diamine to modify OH-PCL-yne to Boc-NH2-PCLyne. After BOC deprotection, the modified amine end group was reacted with the activated carbonyl group of DOX to form DOX-PCL-yne as the hydrophobic complex. To prepare α,ω -p-toluenesulfonyl-yne-poly(ϵ caprolactone) (OTs-PCL-yne), a reported procedure was followed (Lancuški et al., 2012). Briefly, OH-PCL-yne (5 g, 1.5 mmol) was dissolved in 25 mL of dichloromethane in a round-bottom flask. 4-Toluenesulfonyl chloride (TsCl) (5 eq, 1.4 g) and triethylamine (5 eq, 0.750 g) were dissolved in 15 mL of DCM, added to the solution dropwise, and let to stir for about 30 h at 25 °C. The mixture was then washed with a saturated solution of NaCl, HCl (1 M), and H2O and the organic phase was separated using a separating funnel. The solution was then dried over MgSO4, filtered, and concentrated using a rotatory evaporator. The remaining product containing OTs-PCL-yne was dissolved in a minimum amount of dichloromethane, precipitated in cold diethyl ether, and freeze-dried (Tajhizat Sazan Pishtaz, Iran).

Ethylenediamine was employed as the coupling agent to conjugate DOX to yne-PCL. First, one of the two amine end groups of ethylene-diamine was protected with Boc. The other free amine was then bound to yne-PCL-OTs to convert it to yne-PCL-NH2. Yne-PCL-NH2 was then reacted with the free carboxyl group of Dox. Di-tert-butyldicarbonate (Boc2O) (10 g, 45 mmol) was dissolved in 25 mL of 1,4-dioxane, added dropwise to the solution of ethylenediamine (EDA) (21.5 g, 358 mmol) in 1,4-dioxane (20 mL), and kept stirring at 25 °C for 24 h. The solvent was then evaporated and the mixture was washed with 30 mL of distilled water so that insoluble bis(N,N'-tert-butyloxycarbonyl)-1,2-diaminoethane (Boc-EDA-Boc) precipitated and was separated via filtration. Water-soluble tert-butyl-N-(2-aminoethyl) carbamate (Boc-EDA) was extracted three times with 40 mL of CH₂Cl₂. The organic phase was dried over MgSO4 and concentrated to yield Boc-EDA as a colorless oil.

Tosyl-activated PCL-yne (2 g, 0.57 mmol) was dissolved in DMSO and gradually added to the mixture of Boc-EDA (4 eq., 370 mg) in DMSO, heated up to 70 °C, and let to stir for about 48 h. After the completion of the reaction, trifluoroacetic acid (TFA) (1 mL) was added to the mixture and kept stirring overnight at 25 °C to deprotect terminal amine group. The solvent was freeze-dried and the remaining crude was washed several times with distilled water to wash out the non-reacted EDA and TFA from NH2-PCL-yne. Doxorubicin was conjugated to yne-PCL-NH2 via imine reaction between the amine group of NH₂-PCL-yne and the carbonyl group of DOX. The prepared NH₂-PCL-yne (100 mg, 28 Âμmol) was reacted with DOX (48 mg, 88 μmol) in the presence of EDC (13.7 mg, $88 \mu mol$) and NHS (10.31 mg, $88 \mu mol$) as the carbonyl activator in DMSO medium. This mixture was stirred for about 48 h at 25 °C. It was then freeze-dried and washed several times with distilled water to remove the remaining unreacted reagents from the produced DOX-PCL-yne. Afterward, it was freeze-dried and kept in inert conditions for further reactions. In all steps, the pH of the reaction was controlled to be basic in order to prevent imine hydrolysis and the unwanted release of DOX.

2.1.4. Conjugating hydrophobic and hydrophilic sides on the core NP 2.1.4.1. Conjugating hydrophilic side (Acl-sPEG) on N₃-SPION-SH. Acl-sPEG was conjugated to N3-SPION-SH via thiol-ene click reaction (Bradley et al., 2016). Here, to prevent azide photodecomposition, the thermal radical initiator was used to perform the thiol-ene click reaction (Goddard-Borger et al., 2012). Briefly, N₃-SPION-SH (0.1 mmol –SH) was dispersed in degassed MeOH (5 mL) containing Acl-sPEG (0.1 mmol, 95 mg). The degassed MeOH (2 mL) solution of azobisisobutyronitrile (AIBN) (1 μ mol, 0.18 mg) was added dropwise to the main reaction medium while it was refluxing at 70 °C under an inert condition in a dark place far from any light source. Stirring continued for 48 h. The sPEG conjugated NPs (N3-SPION-sPEG) were then collected using external magnetic field and washed three times with MeOH.

2.1.4.2. Conjugating folic acid (FA) onto N3-SPION-sPEG. Folic acid

conjugation was prepared by carbodiimide coupling chemistry. The carboxyl group of FA was first activated (Li et al., 2017) and then reacted with free hydroxyl end groups of the sPEG. Briefly, FA (300 mg, 680 mmol), dicyclohexylcarbodiimide (DCC) (93 mg), N-hydroxysuccinimide (NHS) (77 mg), and triethylamine (0.5 mL) were dissolved in dried DMSO (10 mL), added to a one-neck flask, and stirred overnight at 30 $^{\circ}$ C in a dark place. It was then filtered to remove the produced dicyclohexylurea and added dropwise to a mixture of 100 mL of cold acetone and anhydrous diethyl ether (1:2). The precipitated yellow product was separated and washed several times with anhydrous diethyl ether and then freeze-dried.

The resulting NHS-ester of folic acid (100 mg, 0.185 mmol) was dissolved in DMSO. A dispersion of N3-SPION-sPEG (0.89 mg, 0.062 mmol) in 5 mL DMSO was added to the solution of NHS-ester of folic acid in a foil-covered round-bottom flask, and the reaction was continued overnight at 25 °C. Afterward, the precipitate was separated using an external magnetic field and washed in triplicate with DMSO and DCM to remove the remaining excess amount of folic acid and regents. N₃-SPION-sPEG-FA NPs were then sonicated three times in deionized water, acetone, and ethanol, respectively, and magnetically separated and vacuum-dried at 25 °C for 24 h.

2.1.4.3. Conjugating the hydrophobic side (DOX-PCL-yne) on N_3 -SPION-sPEG-FA. DOX-PCL-yne was conjugated to N_3 -SPION-sPEG-FA via alkyne-azide cycloaddition (CuAAC) click reaction catalyzed by CuBr/PMDETA. N3-SPION-sPEG-FA (0.93 mg, 50 μ mol azido groups) was dispersed in 30 mL DMSO containing DOX-PCL-yne (173 mg, 50 μ mol) and PMDETA (11 μ L, 50 μ mol). The mixture was rigorously degassed to remove oxygen from the medium. CuBr (7.17 mg, 50 μ mol) was introduced into the mixture, the reaction flask was sealed, and the reaction continued for 72 h at 25 °C. After the completion of the reaction, DOX-PCL-SPION-sPEG-FA NPs were collected using an external magnetic field and washed several times with DMSO and MeOH.

2.2. Preparing Janus, monolayer, and FA-free Janus nanoparticles

Five types of NPs were prepared in this study: drug-conjugated Janus NP (DOX-PCL-SPION-sPEG-FA), Janus NP (PCL-SPION-sPEG), two simple monolayer NPs, i.e. SPION-sPEG-FA (M1) and DOX-PCL-SPION (M2) which consist of a layer of folic acid-conjugated sPEG and DOX-conjugated PCL, respectively, and FA-free Janus NPs (DOX-PCL-SPION-sPEG). The synthesis process of Janus NP (PCL-SPION-sPEG) was most similar to the described preparation methods used to produce the drug-conjugated Janus NP (DOX-PCL-SPION-sPEG-FA). The magnetic core was synthesized, waxed through the Pickering emulsion method, half-coated by MPTES, and then dewaxed using the solvent exactly as described. N3-APTES was then anchored on the free side of the core particle. Then, Acl-sPEG was conjugated to the core via thiolene click reaction. For Janus NP, HO-PCL-yne was utilized as the hydrophobic side and sPEG was not modified with folic acid molecules (Fig. S1). Simple Janus NPs were prepared to investigate the surfactant properties of NP's platform and in-vitro toxicity evaluation.

To prepare M1 (SPION-sPEG-FA), SPIONs were modified with MPTES and then Acl-sPEG was conjugated on the NPs. Folic acid was then grafted to sPEG as described in previous sections (Fig. S2). For M2 (DOX-PCL-SPION) preparation, SPIONs was modified with N3-APTES and DOX-PCL-yne was grafted to the particle via azid-yne click reaction as explained in previous sections (Fig. S3). These particles were used in in-vitro toxicity evaluation and TGA analysis.

FA-free Janus NPs were prepared from conjugating DOX-PCL-yne on $\rm N_3\text{-}SPION\text{-}$ sPEG without attaching folic acid to $\rm N_3\text{-}SPION\text{-}$ sPEG. These particles were used in in-vitro cell uptake evaluation to determine the role of FA in NPs active targeting.

2.3. In vitro tests

2.3.1. In vitro release studies of Janus NP

In order to detect the drug release behavior of drug-conjugated Janus NPs at different pH values, 1 mg of NP was dispersed in 10 mL of freshly made phosphate buffer solutions at three pH values (4, 6.2, and 7.4). The mixture was let to stir at 200 rpm and 37 $^{\circ}$ C. At distinct intervals, the NPs were separated from the media using an external magnetic field and the media was replaced by the proper solution. The DOX content of the samples taken from the experiment was measured by UV–Vis spectroscopy at 495 nm, according to the calibration curve of DOX in the same pure solution of each pH values.

2.3.2. Cytotoxicity evaluation

The rat C6 glioma cell line was obtained from the National Cell Bank of Iran (NCBI), Pasteur Institute, Tehran, Iran. Cells were cultured in 90% Dubelco's modified essential medium (DMEM)/10% fetal bovine serum (FBS; Gibco, USA), 100 U/mL of penicillin, and 100 g/mL of streptomycin in a humidified incubator, at 37 °C and 5% CO2.

The toxicity of DOX, drug-conjugated Janus NP, Janus NP, (M1), and (M2) NPs on Rat C6 glioma cell line was evaluated through 3-(4,5-Dimethylthiazol-2-yl)-2,5-diphenyltetrazolium-bromide (MTT) assay. Briefly, 1×10^4 rat C6/well were seeded in 96-well plates and incubated overnight. The concentrations of 50, 100, 200, 500, and $1000\,\mu g$ of each NP were dispersed in $100\,\mu L$ of DMEM supplemented with 10% FBS and added to 6 wells containing the seeded cells. In the following 24 h, the medium was removed and replaced with 100 µL of a 0.5 mg/mL MTT solution (Sigma, USA). After 4 h, purple formazan crystals were dissolved in 100 µL of isopropanol (Merck, Germany) by incubation at 37 °C for 15 min. The absorbance of each well was measured by a multi-well microplate reader (Statfax 2100, USA) at 545 nm and normalized to the control measurement. Prior to in vitro NP evaluations, optimum pH value and time in which rat C6 cells remained alive in the acidic medium was determined. These MTT assays were performed as explained in this section. Time variance was between 6 and 48 h for the pH values of 5.8, 6, 6.2, 6.8, and 7.4.

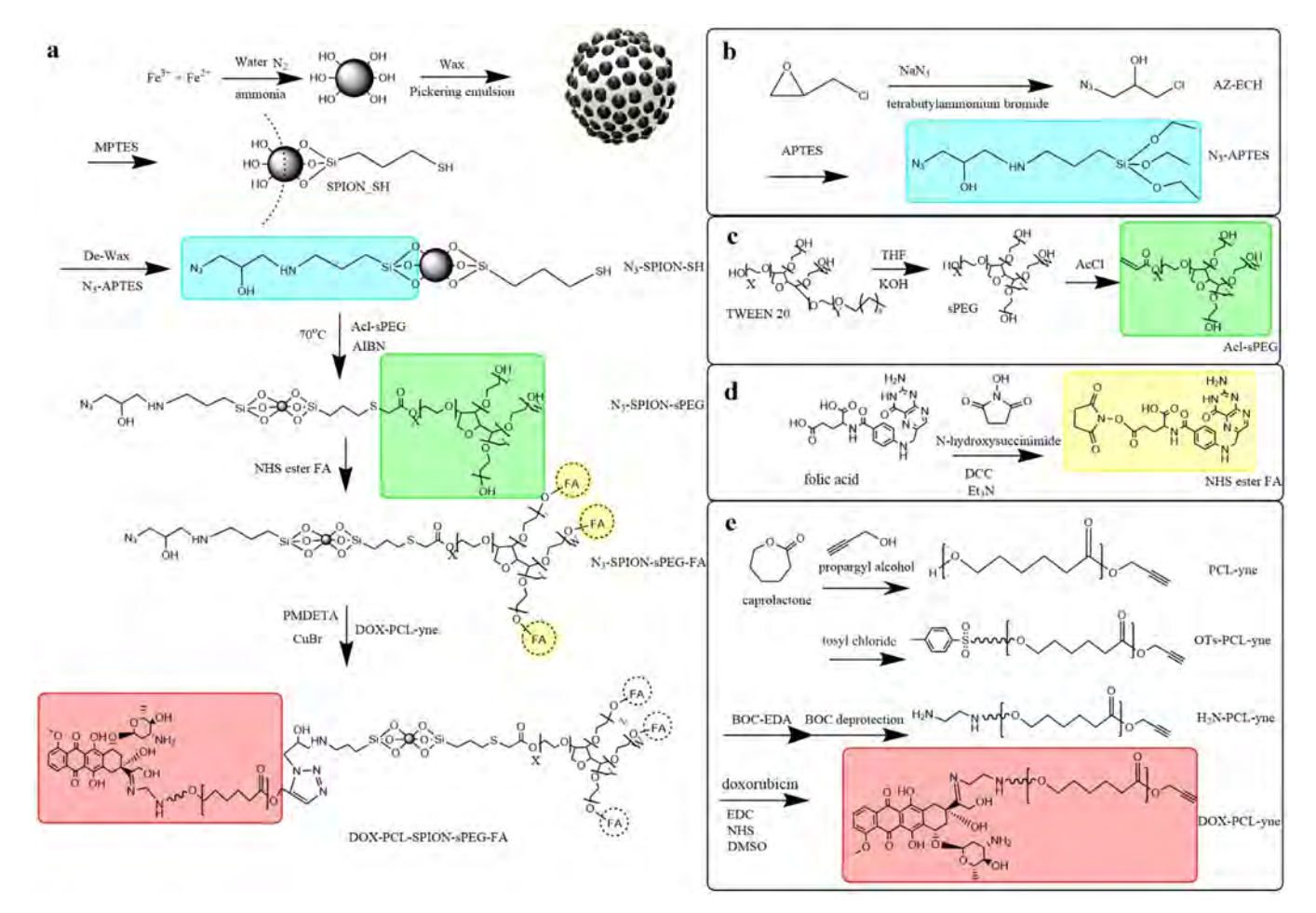
2.3.3. Cell uptake study

For qualitative cell uptake study, C6 glioma cells were seeded on sterile 18 mm round glass coverslips at a concentration of 1×10^4 cells/coverslip and incubated overnight. Seeded cells were then incubated with the dispersion of 100 µg drug-conjugated NPs and FA-free Janus NPs in 0.5 mL of 90% DMEM/10% FBS medium for 1, 3, and 5 h at 37 °C. After determined intervals, cells were washed with PBS and fixed by paraformaldehyde for 30 min. Cells were then stained using propidium iodide (PI) via 15 min of incubation, washed three times with PBS, and observed by confocal laser scanning microscopy Leica TCS SP5 II with excitation wavelength at 488 nm.

For the quantitative study, the fixed cells on 6 coverslips from the previous phase were incubated with bovine serum albumin (BSA) at $4\,^\circ\text{C}$ for 1 h and then washed with PBS several times to take out non-internalized NPs. The supernatant was removed and the cells were lysed using 0.5 mL of 90% DMSO/10% PBS overnight at 25 $^\circ\text{C}$. The lysate mixture was collected and NP concentration was measured by UV–Vis spectroscopy at 495 nm, according to the calibration curve of DOX in the NP-free lysate mixture. Cell uptake efficiency is reported as the percentage of internalized NPs.

3. Results and discussion

We prepared Janus SPIONs decorated with FA and DOX in order to target cancerous cells and deliver chemotherapy drugs. The main focus of this work was on producing a particle with the potential to pass the BBB due to its surfactant properties. The work was divided into two parts, the synthesis, and characterization of the Janus NPs and the in vitro evaluation of these particles.



Scheme 1. Schematic presentation of drug-conjugated Janus NP synthesis steps: a) core preparation and conjugation of the hydrophilic and hydrophobic side, b) preparation of N_3 -APTES, c) Acl-sPEG synthesis, d) activation of folic acid and e) the hydrophobic side preparation. Schematic wave bond indicates that the conjugating functional group is connected to the last hydroxyl group of PCL chain.

Superparamagnetic iron oxide NPs were prepared via the co-precipitation method which is a simple, easy, and cost-effective method for magnetic NP preparation (Scheme 1).

Black precipitated SPIONs were collected with the external magnetic field and their surface nature was characterized by FT-IR analysis (Fig. 1a). The broad peak at $3200\,\mathrm{cm}^{-1}$ is attributed to the stretching vibration of Fe-OH functional groups on the surface of the magnetic NP and the peak at $588\,\mathrm{cm}^{-1}$ indicates the Fe-O bonds of SPIONs.

Janus NPs were prepared through a Pickering emulsion. A large amount of Janus NPs can be prepared through this easy, fast, and inexpensive technique. Since the melting point of paraffin wax granules is about 62 °C, gradually adding wax granules into a mixture of dispersed SPION NPs in water with a higher temperature would melt the wax. Hydrophilic SPION NPs would act as an emulsifier that settles in the interface of two liquid phases. Melted wax is shredded into small particles through vigorous stirring and is coated by the SPION NP. This would stabilize wax emulsion in the water medium. Therefore, when the mixture is suddenly cooled down, the light brownish solid particles of SPION-coated wax called colloidosomes 28 would float on the surface of water due to wax density (Fig. 2).

These colloidosomes express a magnetic behavior and are absorbed into a magnetic field because of magnetite NPs trapped as a layer on the surface of waxed NPs. The wettability of SPION NPs plays a key role in this technique. Drying SPION NPs before this stage can affect wettability and may result in failure. Trapping the SPION NPs on the surface of wax particles would mask one side of these NPs. The free unshielded side of the particles can be chemically modified with proper agents and

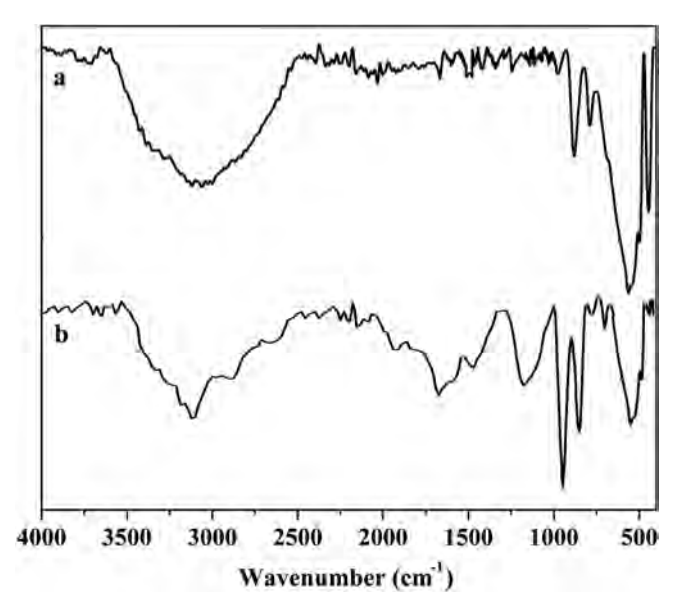


Fig. 1. The FT-IR spectrum of a) bare SPION and b) SPION-SH.

groups to form half-coated particles.

The free side of trapped SPIONs was decorated with (3-mercapto-propyl) trimethoxysilane (MPTES). The FT-IR spectra of MPTES-modified SPIONs (Fig. 1b) show the new peaks added to the characteristic

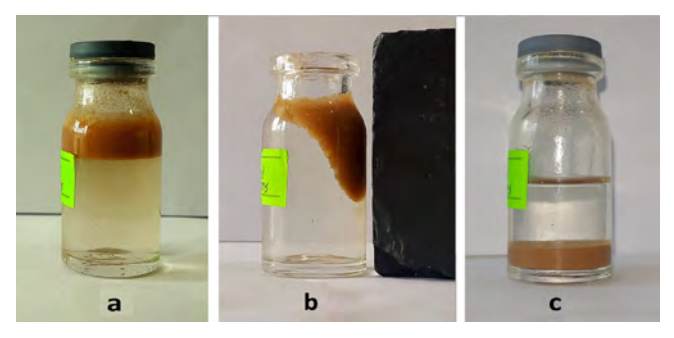


Fig. 2. Waxed SPION colloidosomes a) float on the surface of the water, b) attracted to the external magnetic field, and c) precipitated in ethanol.

peaks of bare NPs. Peaks at 1032 and $1115\,\mathrm{cm}^{-1}$ are attributed to Si-O stretching, and the peak at $3127\,\mathrm{cm}^{-1}$ is related to the carbon-hydrogen bonds absorption (CH₂) of MPTES.

The attached silane group moles were theoretically estimated from simple calculations (McCarthy et al., 2012) listed in Table 1. SPION radius was considered to be around 15 nm. As the Janus NPs are half-modified by silane groups, the moles of silane per sample were divided by 2 to measure the moles of silane per 1 g of Janus NP, which equals 0.3437.

SPION-SH particles were then washed off the wax and the other bare side of the particles was modified with azidated triethoxysilane. Azidated triethoxysilane (N₃-APTES) itself was prepared from the reaction of azidated epichlorohydrin (1-chloro-2-hydroxy-3-azidopropane) (AZ-ECH) and (3-aminopropyl) triethoxysilane (APTES). Azidated epichlorohydrin was prepared from epichlorohydrin and sodium azide in the presence of a phase-transfer catalyst. The FT-IR spectrum of AZ-ECH is depicted in Fig. 3a. The strong absorption at $2087\ {\rm cm}^{-1}$ attributed to the azide group and a characteristic peak at $1267\ {\rm cm}^{-1}$ is related to the CH₂-Cl bond. AZ-ECH was then reacted with APTES to form N₃-APTES.

FT-IR spectrum of azidated APTES (Fig. 3b) compared to AZ-ECH spectrum that shows the appearance of the $1031~\rm cm^{-1}$ and $1116~\rm cm^{-1}$ peak related to the Si–O–H and Si–O–Si bonds, as well as, remaining of the strong peak at $2096~\rm cm^{-1}$ related to the azide group confirms the attachment of AZ-ECH to APTES.

SPION-SH was modified with N_3 -APTES to form N3-SPION-SH. After producing the Janus core particle (N_3 -SPION-SH), hydrophilic and hydrophobic sides were prepared. The hydrophilic side (FA-sPEG) was synthesized in multiple steps. First, sPEG was obtained from the hydrolysis reaction of polysorbate Tween 20 in refluxing alkaline THF. The hydrolysis reaction was confirmed by FT-IR spectrum (Fig. 3c). A distinct stretching peak related to the carbonyl group of lauric acid at $1730~{\rm cm}^{-1}$ disappears, meaning that this group is successfully separated through hydrolysis. sPEG has 4 hydroxyl terminal groups only one

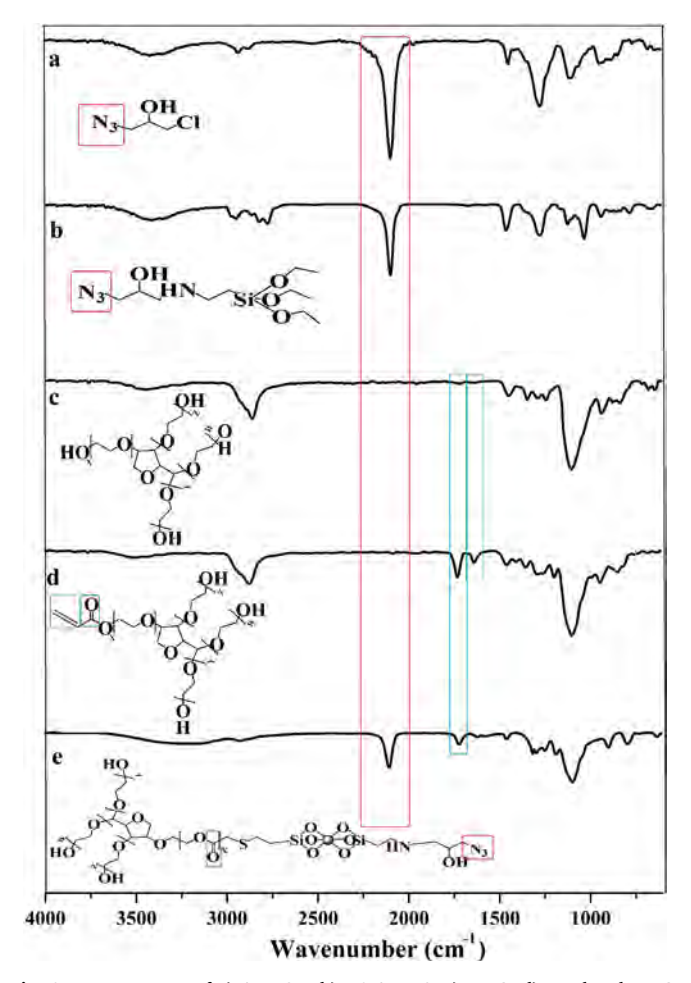


Fig. 3. FT-IR spectra of a) AZ-ECH, b) N3-APTES, c) sPEG, d) acrylated sPEG, and e) N_3 -SPION-sPEG.

of which was acrylated in the next step. FT-IR spectrum (Fig. 3d) demonstrates the characteristic peaks of sPEG as well as two new peaks at 1633 and 1724 cm $^{-1}$, which respectively indicate C = C and carboxylic acid C=O stretching vibration in Acl-sPEG. The intensity of the hydroxyl stretching vibration peak around 3000-3500 cm $^{-1}$ was reduced due to the acrylation of the hydroxyl group.

Acl-PEG was then conjugated to MNP core via thiol-ene click reaction between terminal thiol groups on N3-SPION-SH and Acl-PEG to form N_3 -SPION-sPEG. This was characterized by Fourier-transform infrared spectroscopy (Fig. 3e). By comparing this spectrum with bare and silanized MNPs, sPEG-modified particles exhibit new peaks at

Table 1
Theoretically estimation of the silane groups' moles for 1 g Janus nanoparticle, the mass of drug-conjugated Janus NPs produced from 1 g NP, and Dox per gram of drug-conjugated JNPs.

Definition	Value	Equation	Amount
Volume per nanoparticle	V_{NP}	$(4/3 \pi r^3)$	$1.41 \times 10^4 \text{ nm}^3$
Surface area per nanoparticle	S_{NP}	$(4\pi r^2)$	$2.82 \times 10^{3} \text{nm}^{2}$
Density	d	-	$8.4 \times 10^{-25} \text{g/nm}^3$
Mass per nanoparticle	M_{NP}	$V_{NP} \times d$	1.19×10^{-20} g
Surface area per silane*	S_{silane}	-	0.4 nm ²
Number of silanes per nanoparticle*	#Si _{NP}	$(S_{NP}/S_{Silane}) \times 0.7$	4.93×10^{3}
Number of nanoparticles per gram	#NP _{Sample}	M_{Sample}/M_{NP}	8.4×10^{19}
Number of silanes per gram	#Si _{Sample}	$\#NP_{Sample} \times \#Si_{NP}$	4.14×10^{23}
Moles of silane per gram	N _{Si/Sample}	#Si _{Sample} /N _A	0.6874
Moles of silane per gram of Janus nanoparticle	N _{Si/Janus} Sample	$N_{Si/Sample}/2$	0.3437
Mass of drug-conjugated JNPs produced from 1 g nanoparticle	M _{drug-conjugated} JNP	$\Sigma(M_{reagents} \times N_{Si/Janus\ Sample})$	2065 g

^{*} Values have been obtained from the literature (McCarthy et al., 2012).

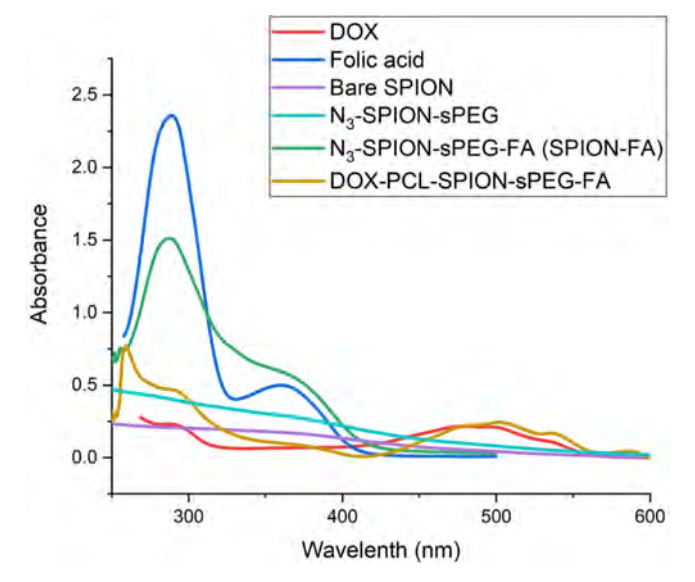


Fig. 4. UV absorption of folic acid, Doxorubicin, bare SPION, N3-SPION-sPEG, N3-SPION-sPEG-FA, and DOX-PCL-SPION-sPEG-FA.

1601, 1093 and 2923 cm⁻¹, attributed to C=O steric, C-O etheric, and C-H bond stretching, respectively, and the wide peak around 3100–3400 cm⁻¹ indicates O-H bond stretch from conjugated sPEG. 1035 and 1117 cm⁻¹ peak are related to the Si-O-H and Si-O-Si bonds. Strong absorption at 2102 cm⁻¹ is attributed to the azide group that remained unchanged in this spectrum. The strong peak at 1601 cm⁻¹ can be related to secondary N-H bend. This can be considered as an evidence for sPEG conjugation on the surface of NPs via click reaction.

Folic acid was then conjugated to previously prepared N_3 -SPION-sPEG via carbodiimide coupling chemistry. The carboxyl group of FA

was first activated with DCC and NHS and then attached to terminal hydroxyl groups of PEG in N_3 -SPION-sPEG. The characteristic UV absorbance of folic acid at 285 and 363 nm was used to verify their attachment to particles. As illustrated in Fig. 4, these two characteristic peaks were also observable for high molecular weight SPION-FA.

The UV spectra of folic acid, Doxorubicin, bare SPION, N₃-SPION-sPEG, N₃-SPION-sPEG-FA, and DOX-PCL-SPION-sPEG-FA were shown in Fig. 4.

The prepared N_3 -SPION-sPEG-FA was then heterogeneously modified with the hydrophobic DOX-PCL-yne polymer. Hydrophobic side synthesis began with the propargyl alcohol-initiated ring-opening polymerization of ϵ -caprolactone. Proton nuclear magnetic resonance (1 H NMR) was employed to investigate the chemical composition of HO-PCL-yne (Fig. 5-1).

The methylenic protons of the PCL chains in CDCl $_3$ as a solvent were observed as multiplets at $\delta=4.05$ (b), $\delta=1.55$ (c, e), $\delta=1.30$ (d) and $\delta=2.3$ (f) ppm. The shifts at $\delta=3.37$ (h) and $\delta=4.6$ ppm (g) indicate terminal acetylene proton and two methylene protons in propargyl end group. The molecular weight was then calculated from the area ratio of acetylene (h) and methyl-related peaks. The molecular weight of PCL was calculated to be about 3500 g/mol.

Ethylenediamine was utilized as a proper crosslinker to conjugate DOX to HO-PCL-yne. The hydroxyl end group of PCL was first activated by tosyl chloride and then reacted with the free amine group of tertbutyloxycarbonyl (Boc)-protected ethylene diamine to make Boc-NH₂-PCL-yne (Scheme 1e). After BOC deprotection, the modified amine end group was reacted with the activated carbonyl group of DOX to form DOX-PCL-yne as the hydrophobic complex. The prepared OTs-PCL-yne, NH₂-PCL-yne, and DOX-PCL-yne were characterized by ^1H NMR (Fig. 5-2, 5-3 and 5-4). In addition to the signals related to HO-PCL-yne, new peaks appeared specifically for each compound. Two significant doublet $\delta=7.8$ (i) and $\delta=7.2$ (j) are related to tosyl groups in OTs-PCL-yne which are added to the HO-PCL-yne spectrum and omitted in the next spectrum related to NH₂-PCL-yne. Instead of these two omitted

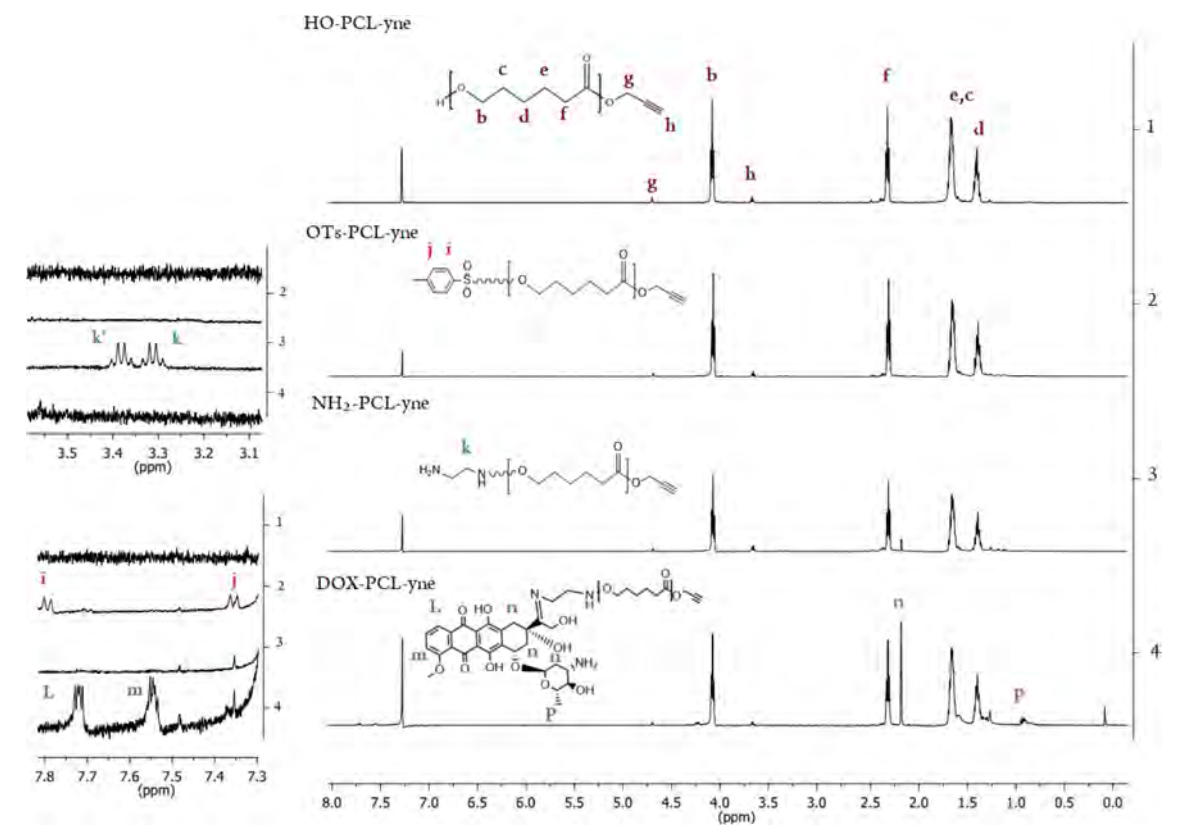
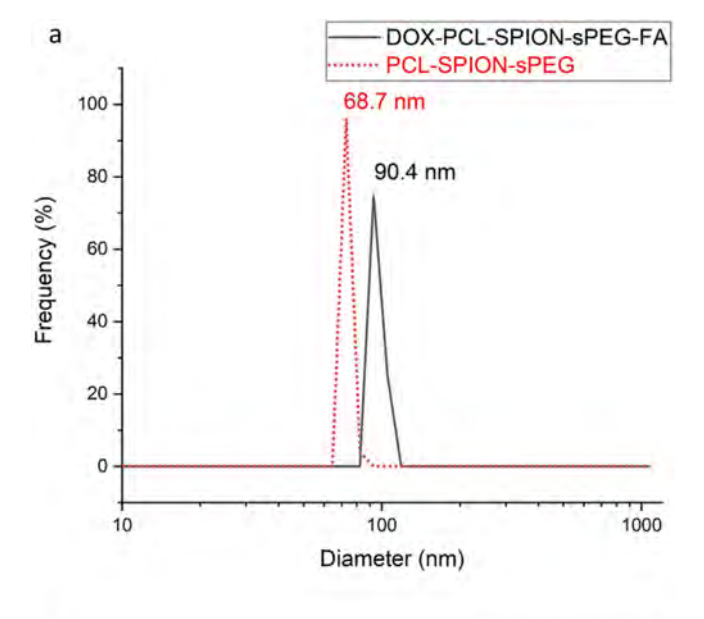


Fig. 5. 1H NMR spectrum of 1) HO-PCL-yne, 2) OTs-PCL-yne, 3) NH2-PCL-yne and 4) DOX-PCL-yne.



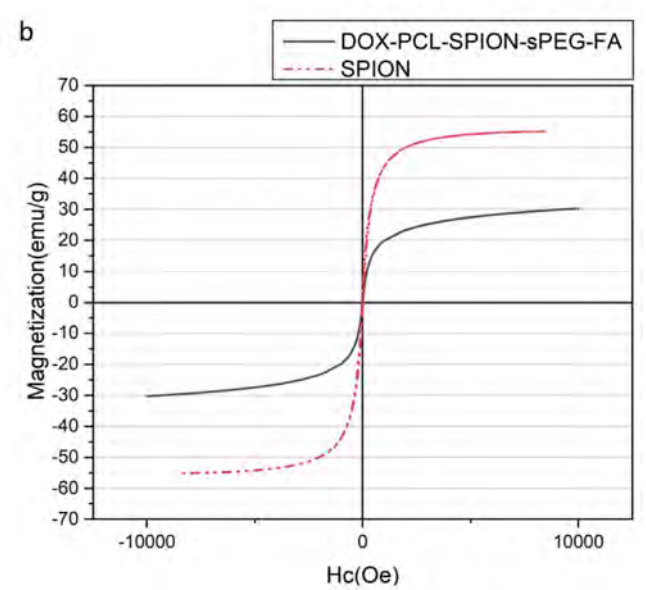


Fig. 6. a) Size distribution of drug-conjugated Janus NP, b) magnetization properties of bare SPIONs and drug-conjugated Janus NP.

peaks, two multiplets have appeared at $\delta=3.3$ and $\delta=3.4$ (k) indicates the methylenic protons adjacent to the amine groups of attached ethylenediamine.

In the 1H NMR spectrum of DOX-PCL-yne, compared to previous spectra, multiple new signals are obvious at $\delta=7.72$ (L), $\delta=7.55$ (m), $\delta=2.2$ (n), $\delta=0.9$ (p) which are indicators for DOX attachment. DOX-PCL-yne was then conjugated to N_3 -SPION-sPEG-FA via alkyne-azide cycloaddition (CuAAC) click reaction, catalyzed by CuBr-PMDETA. The conjugation of DOX-PCL-yne to N_3 -SPION-sPEG-FA was examined using UV–Vis spectroscopy (Fig. 4). FA and DOX had characteristic UV absorption at around 280 nm 495 nm, respectively.

The size distribution of drug-conjugated Janus NP and Janus NP in aqueous solution was measured by DLS (Fig. 6a). The mean size of Janus NP and the drug-conjugated Janus NP equals 68.9 and 90.4 nm, respectively. The size of NPs plays a key role in drug delivery. NPs must be small enough to penetrate through barriers and tumor tissue but large enough to have a proper retention effect (Patel and Patel, 2017).

The presence of an external magnetic field can magnetize superparamagnetic iron oxide NPs. These particles lose their magnetization by the removal of the external magnetic field. This superparamagnetism phenomenon can be used for magnetic hyperthermia and targeted drug delivery. The magnetization variations of prepared drug-conjugated Janus NPs and bare SPIONs are presented in Fig. 6b. The saturation magnetization value of drug-conjugated Janus NP is about 30 emu/g at 25 °C, compared to the saturation magnetization value of bare SPION that is about 55 emu/g at 25 °C. On the other hand, the magnetic properties of NPs would facilitate product purification and separation through the synthetic process. Comparing bare and Janus NPs, the saturation magnetization value has decreased in coated Janus NPs. This is due to the grafted polymer shell on the surface of NPs that affects the magnetization properties. It has been reported that sPEG-coated SPIONs have higher saturated magnetization values compared with linear PEGcoated SPIONs (Khoee et al., 2017b).

The TEM images of Janus NPs (Fig. 7) indicate particles with two different sides. In Fig. 7a, SPIONs which have been half-coated with the sPEG polymer are attached together due to their magnetic attraction. The sPEG coating is recognizable beneath dark SPION cores. As obviously shown in Fig. 7b, Janus NP consists of two separated sides that make them "Janus". The bushy bright side is an sPEG polymer and the darker coat on the other side is PCL.

The weight percent of coated polymers on the surface of NPs can be measured using a thermogravimetric analyzer (Fig. 8). Comparing the TGA results of drug-conjugated Janus NP with M1 and M2, two main mass losses at about 275 and 355 °C are related to sPEG and PCL, respectively. According to TGA curves, the average weight percent of grafted polymers equals 17 W% for the hydrophilic part and 18 W% for

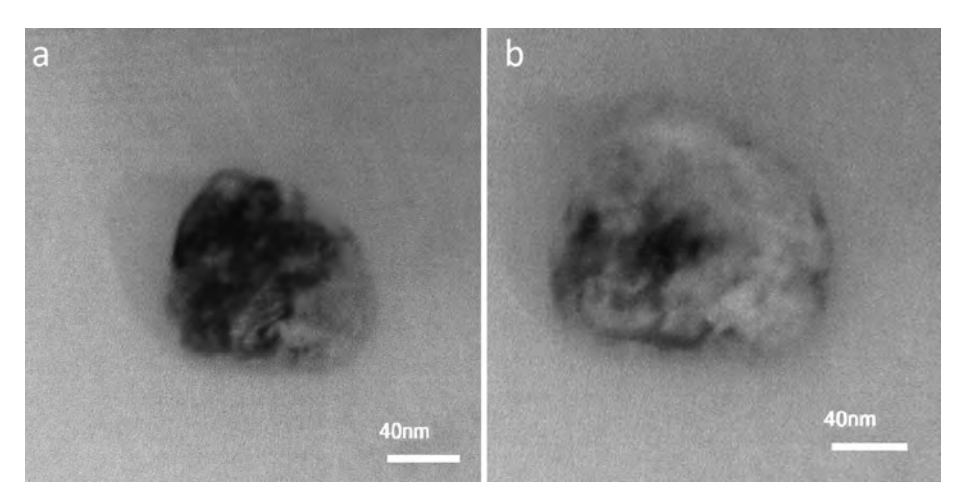


Fig. 7. Transmission electron microscopy picture of a) half-coated SPION particles with a bright coating of sPEG on the back sides b) Janus nanoparticle (PCL-SPION-sPEG) with two distinctly different sides.

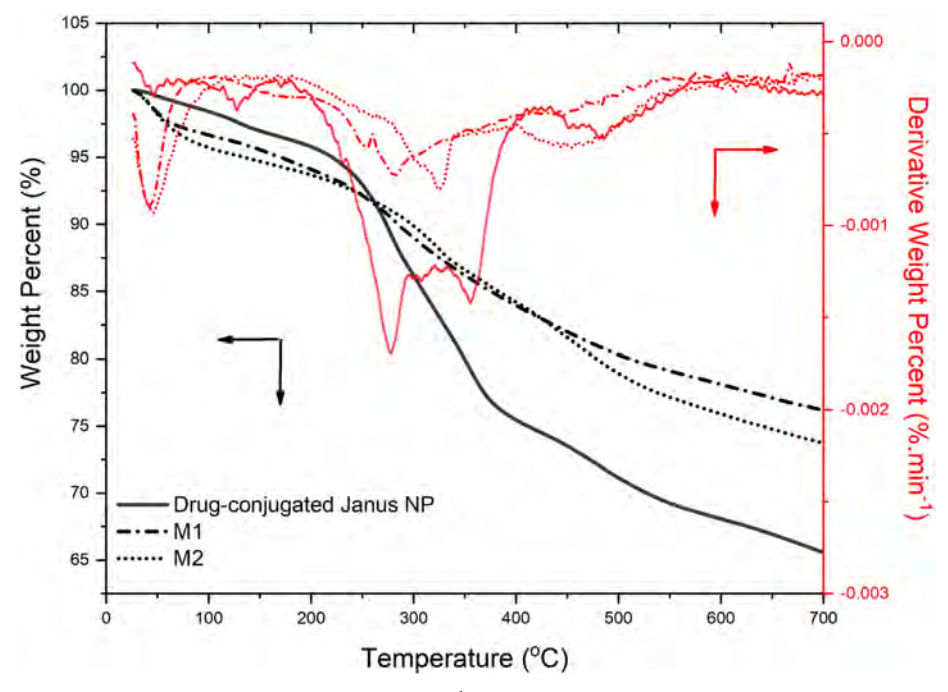


Fig. 8. TGA analysis results at 10 °C min⁻¹ for drug-conjugated Janus NPs, M1, and M2.

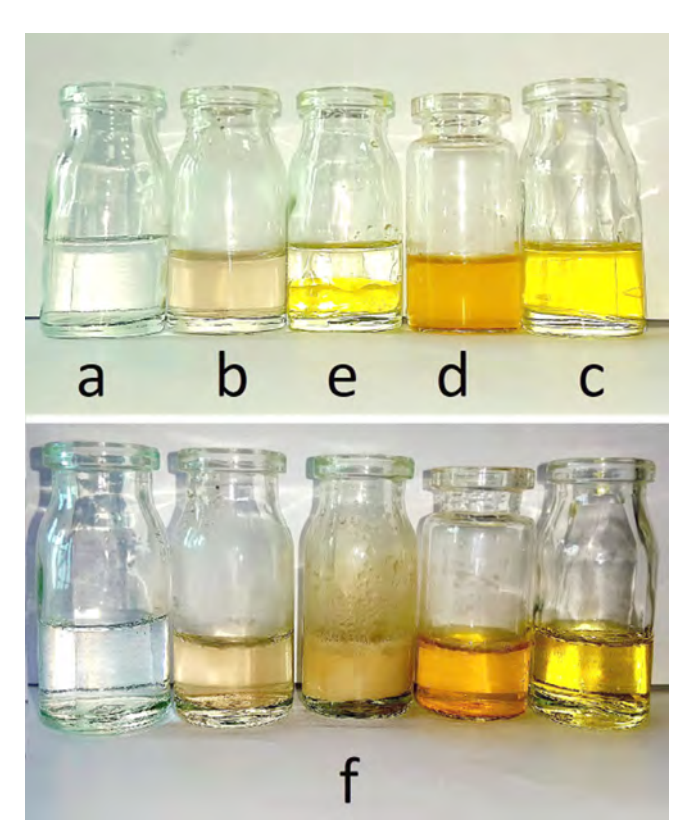


Fig. 9. Surfactant behavior of Janus nanoparticle. a) water, b) dispersed nanoparticles in water, c) dyed CH2Cl2 as the oil phase, d) dispersed nanoparticles in the oil phase, e) oil and water phase mixture, f) nanoparticles dispersed in oil/water mixture, act as a surfactant and made oil in water emulsion.

the hydrophobic part.

In making Janus NPs through the Pickering emulsion technique, the coating ratio of polymers on two sides is highly related to how deep particles penetrate inside the wax balls. The more they move inside the liquid wax before wax congelation, the less they can be modified in the

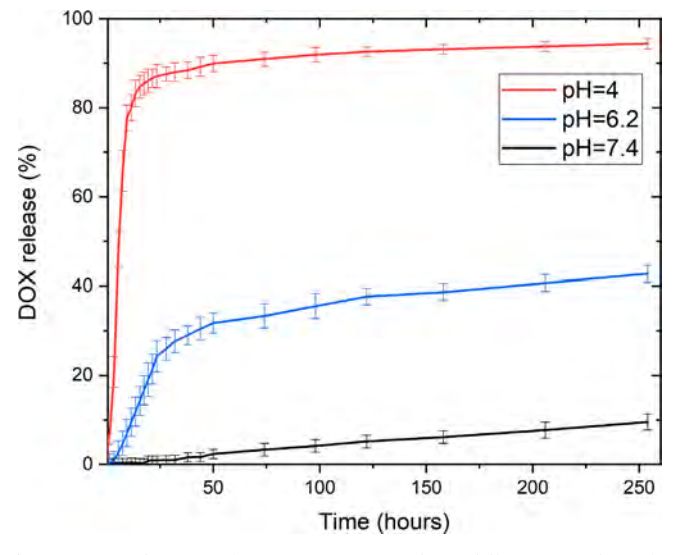


Fig. 10. Drug release rate from Janus nanoparticles at different pH values of 4, 6.2 and 7.4.

first step of polymer coating (sPEG in this work) and the more the second coating polymer (PCL in this work) would be conjugated on the other side of the NP after washing off the wax.

As an amphiphilic Janus NP, PCL-SPION-PEG is desired to have distinct surfactant properties. As illustrated in Fig. 9, a simple visual test was performed to investigate if these NPs can act as a surfactant to make a stabilized oil-in-water emulsion or not.

NPs were well dispersed in both organic (CH_2Cl_2) dyed with Para red) and aqueous (water) phases (Fig. 9b, d). In aqueous solutions, NPs may aggregate such that the hydrophobic sides of NPs would face each other and the hydrophilic sides would face the outer aqueous medium. The inverse mechanism may happen in the organic phase. NPs can aggregate to form a structure that has a hydrophobic outer layer to contact the organic medium. This can be the reason for Janus NPs' well dispersion in both organic and aqueous media. When the organic and aqueous phases are mixed, NPs may place in the interface of these two phases and stabilize the emulsion. The formation of an opaque oil-in-

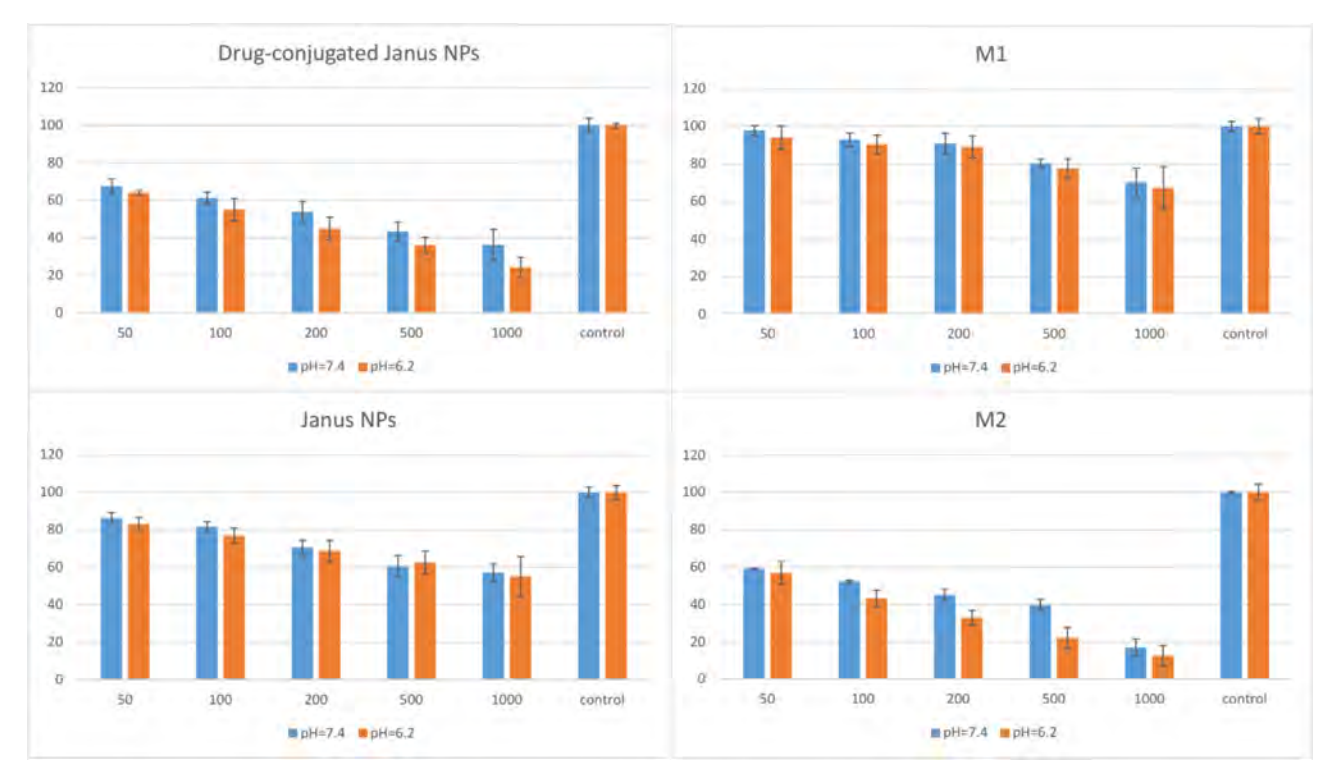


Fig. 11. Cytotoxicity evaluation of drug-conjugated Janus NPs (DOX-PCL-SPION-sPEG-FA), Janus NPs (PCL-SPION-sPEG), SPION-sPEG-FA (M1), and DOX-PCL-SPION (M2) on rat C6 glioma cell-line at pH = 7. 4 and pH = 6.2.

Table 2
IC50 calculation for drug conjugated Janus NPs, Janus NPS, M1, and M2.

Samples pH	1 = 6.2	pH = 7.4
0 - 3 - 3 - 3 - 3 - 3 - 3 - 3 - 3 - 3 -		279.5
1.00		1773.51 12560
1 0	.74	112.411

water emulsion (Fig. 9f) in the presence of Janus NPs is a simple proof for the surfactant properties of these particles.

As the drug release strategy of designed NPs is based on pH-sensitivity, cell toxicity was determined at different pH values and times. According to these data, the optimum pH value and time, i.e. the minimum pH value in maximum time at which the viability of the cells were more than 50%, are pH = 6.2 and 24 h, respectively. Cell viability in this condition is 53.74%.

In order to determine the maximum amount of conjugated drug molecules on the surface of the NPs, precise amount of drug-conjugated Janus NPs was first washed with a basic solution to wash out non conjugated drugs from the NPs and then dispersed them in defined amount of acidic media (pH = 4). The drug release was measured by UV–Vis spectroscopy at 495 nm, according to the calibration curve of DOX in the same acidic solution. Cumulative release of DOX under acidic condition increases sharply at the first 20 h of experiment because of the vast imine bond breakage that releases DOX from NPs. At pH 4, approximately 87.5%, 89.9%, and 94.5% of doxorubicin were released within 24, 50, and 256 h, respectively. The total amount of DOX was released from NPs in 28 days (672 h).

The release study was conducted at two pH values of 6.2 and 7.4 to simulate cancerous and normal cell conditions, respectively (Fig. 10). To measure the drug release in these pH values, drug-conjugated Janus NPs were first washed using basic solution to wash out not conjugated drug molecules which may be loaded between polymer chains or have attached to the conjugated DOX molecules through $\pi\text{-}\pi$ stacking

interactions, to obtain more actual results which represents the accurate amount of conjugated drug molecules.

Under slightly acidic conditions (pH = 6.2), cumulative release of DOX gradually increases within the first 50 h, followed by a steady rate of increase for the rest of the experiment (Fig. 10). At this pH, approximately 25%, 32%, and 42% of doxorubicin were released within 24, 50, and 256 h, respectively. Consuming the steady rate of increase, according to the graph equation, drug release would reach 100% in about $1614\,h$. In contrast to acidic pH, at pH 7.4, only 1%, 2.3%, and 9.5% of doxorubicin were released within 24, 50, and 256 h, respectively.

Comparing the cumulative release of DOX in different media shows that drug release is higher at pH=6.2 at the same time due to the imine bond breakage that occurs under acidic conditions. This indicates that the prepared drug-conjugated Janus NPs are stimuli-sensitive and can be used as a targeting drug delivery system releasing its conjugated drug molecules in the acidic condition of tumors compared to the normal stimuli of blood fluid and normal cells (pH=7.4).

The cytotoxicity quantification of DOX, drug-conjugated Janus NP, Janus NPs, SPION-sPEG-FA (M1), and DOX-PCL-SPION (M2) NPs indicated significant differences in samples' toxicity (Fig. 11, Fig. S4). MTT assay was performed at pH values of 6.2 and 7.4 and various NP concentrations (50, 100, 200, and 1000 μg) for all samples. In the case of drug-conjugated Janus NP and M2, the difference between cell viabilities in two pH values is more distinct due to more drug molecule release at pH = 6.2 because of imine bond breakage, as investigated in the release test. The M1 NP can be considered as nontoxic in these conditions because of its surface modification. M2 toxicity is much higher than drug-conjugated Janus NP due to full DOX-PCL modification all over the NPs, making the DOX concentration twice that of Janus NP

IC50 is calculated for drug conjugated Janus NPs, Janus NPS, M1, and M2 on the basis of their cell viability data (Table.2).

Cell uptake of drug-conjugated Janus NPs was studied via confocal microscopy. Cells were incubated with FA-free and FA-conjugated

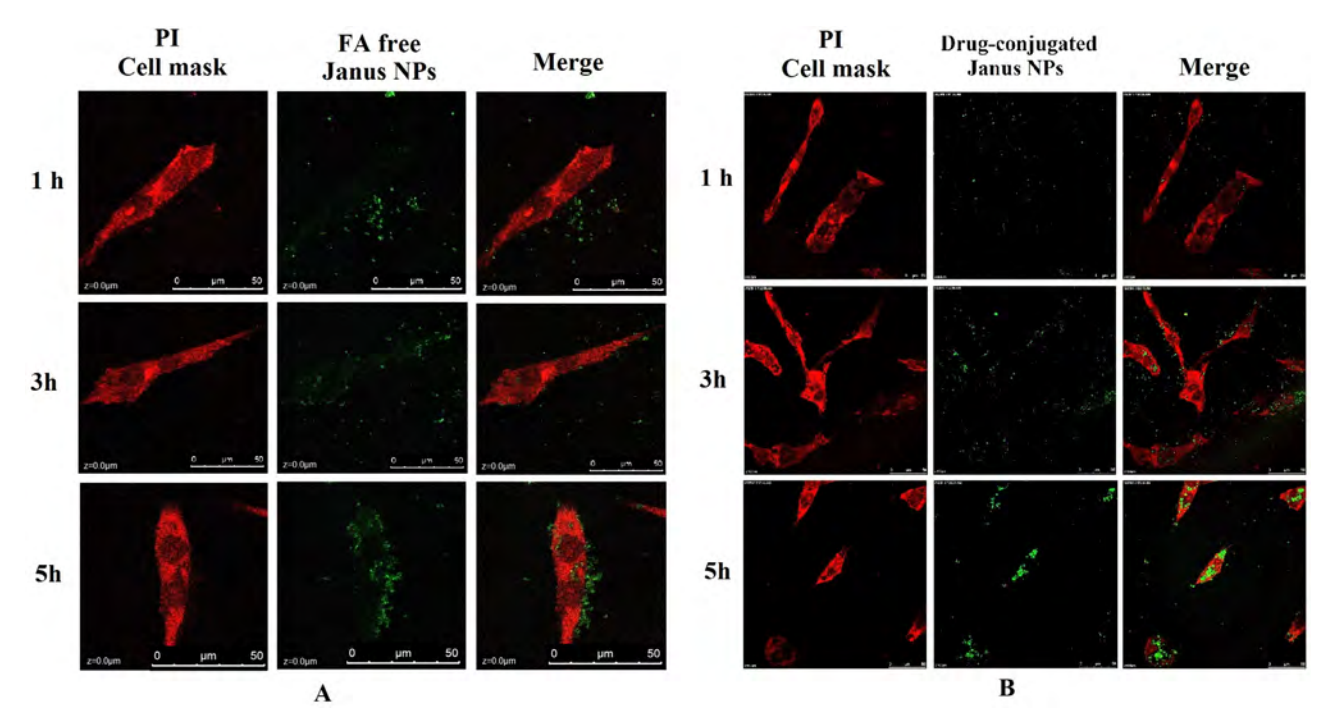


Fig. 12. Confocal microscopic study of time-dependent cell uptake of FA-free drug-conjugated Janus NPs (A) and folate mediated cell uptake of drug-conjugated Janus NPs (B) at the indicated time. Rat C6 glioma cells were stained with PI. The intracellular locations of NPs are observed as green dots.

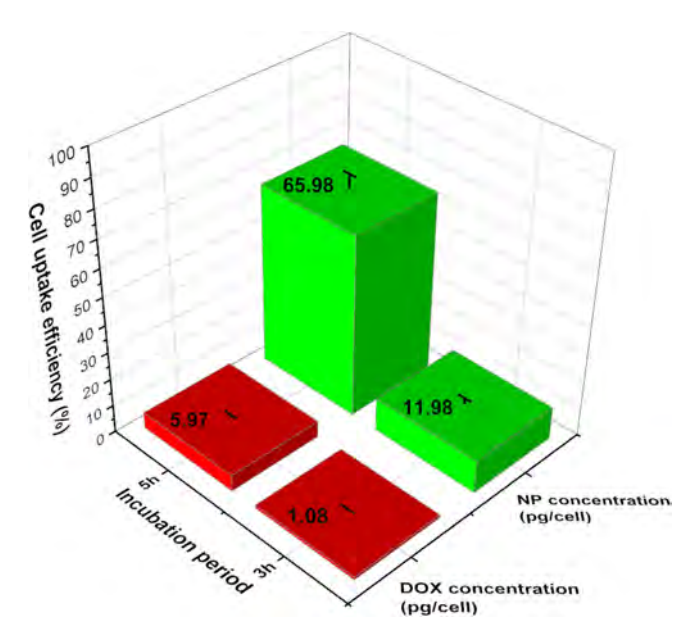


Fig. 13. Quantitative cell uptake study of drug-conjugated Janus NPs. The concentrations of internalized NPs are reported as picogram per cell. N = 6.

Janus NPs (Fig. 12A and B, respectively) at 37 °C for 1, 3, and 5 h and stained by PI to label the cells' nucleic acid. Conjugating folic acid (FA) on PEG can improve the tumor accumulation of nanoparticles (NPs) and intracellular delivery (Hayashi et al., 2013; Oyewumi and Mumper, 2003). In vitro tests were carried out in Rat C6 glioma cells since they are known to express folate receptors (Saul et al., 2003). As compared in Fig. 12, the folate-mediated cell uptake of drug-conjugated Janus NPs (Fig. 12.B) is significantly higher than time-dependent cell uptake of FA-free drug-conjugated Janus NPs (Fig. 12A). Nanoparticles were observed as green dots in confocal images, which are dispersed outside the cells after 1 h incubation. After 3 h, most of NPs have aggregated around the cells' membrane and some has penetrated into the cells. Punctate pattern of NPs internalization indicates the vesicular

endocytosis uptake. Incubating the cells for 5 h resulted in successful cell penetration. Most of the NPs have been uptaken by cells as green fluorescent punctate packages inside the cells (Fig. 12B). Apoptosis pattern of a cell is also observable at only 5 h of cell incubation. After incubating FA-free Janus NPs with C6 cells for 5 h, NPs accumulated on the surface of the cells and only a little percentage of NPs have entered the cells via passive targeting, compared to the cell uptake of drugconjugated Janus NPs after 5 h in which most of the NPs have been uptaken by cells as green fluorescent punctate packages inside the cells.

A quantitative study was carried out to determine the amount of internalized NPs per cell for 6 coverslips. NPs that remained in the medium or attached on the cell membrane was washed off using BSA and the cells were lysed. DOX concentration of the lysate was measured and the NP concentration was calculated using data from Table.1. The concentration of internalized NPs and cell uptake efficiency are not measurable for 1 h incubation because of extremely small amounts of penetrated NPs and detecting limits. The concentration of internalized NPs is much higher in the case of 5 h incubation, which is about 6 times higher compared to the NP concentration in 3 h incubation that matches the microscopy visual data (Fig. 13). Cell uptake efficiency is measured as the percentage of internalized NPs. Cell uptake efficiency was 0.24 and 1.32% for 3 and 5 h of incubation, respectively.

4. Conclusion

Drug-conjugated Janus NPs were prepared on the basis of an amphiphilic Janus NP platform as a potent targeting drug delivery system that can be employed as both stimuli-responsive targeting agent and a magnetic targeting agent. Prepared Janus NPs were decorated with DOX and FA as chemotherapeutic drug and a targeting agent models, respectively. NPs were physicochemically evaluated. Conjugating DOX molecules to the particle may increase drug blood circulation time and, due to the covalent bond between drug and vehicle, fewer drug molecules would release in undesired tissues. The imine bond that grafted the drug to the surface of coating polymer can be hydrolyzed in the acidic condition of tumors and releases the conjugated molecule. In vitro tests proved the pH-dependency of drug release for drug-

conjugated Janus NPs. These drug-conjugated Janus NPs were determined to be vital for rat C6 glioma cell line. The MTT assay was performed in normal and acidic conditions to examine the effects of pH variation on cell viability in the presence of the NPs. It was investigated that drug-conjugated Janus NP is more vital in acidic condition. Quantitative in vitro cell uptake study revealed that after 5 h, NPs have accumulated in the cells in a considerable concentration. Laser confocal microscopy approved the quantitative results and showed internalization pattern of Janus NPs. All these characterizations revealed that prepared Janus NP can be used as a reliable drug delivery platform which can be decorated with different types of therapeutic, targeting, and/or diagnostic molecules with different characteristics to offer an effective multifunctional nanomedicine for patients suffering from cancer.

Appendix A. Supplementary data

Supplementary data to this article can be found online at https://doi.org/10.1016/j.ijpharm.2019.01.020.

References

- Basiruddin, S., Saha, A., Pradhan, N., Jana, N.R., 2010. Advances in coating chemistry in deriving soluble functional nanoparticle. J. Phys. Chem. C 114, 11009–11017. https://doi.org/10.1021/jp100844d.
- Bradley, L.C., Stebe, K.J., Lee, D., 2016. Clickable janus particles. J. Am. Chem. Soc. 138, 11437–11440. https://doi.org/10.1021/jacs.6b05633.
- Ellor, S.V., Pagano-Young, T.A., Avgeropoulos, N.G., 2014. Glioblastoma: background, standard treatment paradigms, and supportive care considerations. J. Law Med. <u>Ethics</u> 42, 171–182. <u>https://doi.org/10.1111/jlme.12133</u>.
- Gao, W., Liu, Y., Jing, G., Li, K., Zhao, Y., Sha, B., Wang, Q., Wu, D., 2017. Rapid and efficient crossing blood-brain barrier: hydrophobic drug delivery system based on propionylated amylose helix nanoclusters. Biomaterials 113, 133–144. https://doi. org/10.1016/j.biomaterials.2016.10.045.
- Goddard-Borger, E.D., Tropak, M.B., Yonekawa, S., Tysoe, C., Mahuran, D.J., Withers, S.G., 2012. Rapid assembly of a library of lipophilic iminosugars via the thiol—ene reaction yields promising pharmacological chaperones for the treatment of Gaucher disease. J. Med. Chem. 55, 2737–2745. https://doi.org/10.1021/jm201633y.
- Hayashi, K., Nakamura, M., Sakamoto, W., Yogo, T., Miki, H., Ozaki, S., Abe, M., Matsumoto, T., Ishimura, K., 2013. Superparamagnetic nanoparticle clusters for cancer theranostics combining magnetic resonance imaging and hyperthermia treatment. Theranostics 3, 366–376. https://doi.org/10.7150/thno.5860. Print 2013.
- Kang, Y.J., Cutler, E.G., Cho, H., 2018. Therapeutic nanoplatforms and delivery strategies for neurological disorders. Nano Converge 5, 35. https://doi.org/10.1186/s40580-018-0168-8
- Khoee, S., Bagheri, Y., Hashemi, A., 2015. Composition controlled synthesis of PCL–PEG Janus nanoparticles: magnetite nanoparticles prepared from one-pot photo-click reaction. Nanoscale 7, 4134–4148. https://doi.org/10.1039/c4nr06590e.
- Khoee, S., Yousefalizadeh, G., Kavand, A., 2017a. Preparation of dual-targeted redox-responsive nanogels based on pegylated sorbitan for targeted and antitumor drug delivery. Eur. Polym. J. 95, 448–461. https://doi.org/10.1016/j.eurpolymj.2017.08.030.
- Khoee, S., Saadatinia, A., Bafkary, R., 2017b. Ultrasound-assisted synthesis of pH-responsive nanovector based on PEG/chitosan coated magnetite nanoparticles for 5-FU delivery. Ultrason. Sonochem. 39, 144–152. https://doi.org/10.1016/j.ultsonch. 2017.04.025.
- Kreuter, J., 2001. Nanoparticulate systems for brain delivery of drugs. Adv. Drug Deliv. Rev. 47, 65–81. https://doi.org/10.1016/S0169-409X(00)00122-8.
- Lallana, E.C., Abrey, L.E., 2003. Update on the therapeutic approaches to brain tumors. Expert Rev. Anticancer Ther. 3, 655–670. https://doi.org/10.1586/14737140.3.5.
- Lancuški, A., Fort, S., Bossard, F., 2012. Electrospun azido-PCL nanofibers for enhanced

- surface functionalization by click chemistry. ACS Appl. Mater. Inter. 4, 6499–6504. https://doi.org/10.1021/am301458y.
- Lee, N., Yoo, D., Ling, D., Cho, M.H., Hyeon, T., Cheon, J., 2015. Iron oxide based nanoparticles for multimodal imaging and magnetoresponsive therapy. Chem. Rev. 115, 10637–10689. https://doi.org/10.1021/acs.chemrev.5b00112.
- Li, L., Jiang, W., Luo, K., Song, H., Lan, F., Wu, Y., Gu, Z., 2013. Superparamagnetic iron oxide nanoparticles as MRI contrast agents for non-invasive stem cell labeling and tracking. Theranostics 3, 595–615. https://doi.org/10.7150/thno.5366.
- Li, W., Tan, G., Zhang, H., Wang, Z., Jin, Y., 2017. Folate chitosan conjugated doxorubicin and pyropheophorbide acid nanoparticles (FCDP-NPs) for enhance photodynamic therapy. RSC Adv. 7, 44426–44437. https://doi.org/10.1039/C7RA08757H.
- Lockman, P., Mumper, R., Khan, M., Allen, D., 2002. Nanoparticle technology for drug delivery across the blood-brain barrier. Drug Dev. Ind. Pharm. 28, 1–13. https://doi. org/10.1081/DDC-120001481.
- Mahmoudi, M., Milani, A.S., Stroeve, P., 2010. Synthesis, surface architecture and biological response of superparamagnetic iron oxide nanoparticles for application in drug delivery: a review. Int. J. Biomed. Nanosci. Nanotechnol. 1, 164–201. https://doi.org/10.1504/IJBNN.2010.034651.
- McCarthy, S.A., Davies, G.L., Gun'ko, Y.K., 2012. Preparation of multifunctional nanoparticles and their assemblies. Nat. Protoc. 7, 1677–1693. https://doi.org/10.1038/nprot.2012.082.
- Munthe, S., Sørensen, M.D., Thomassen, M., Burton, M., Kruse, T.A., Lathia, J.D., Poulsen, F.R., Kristensen, B.W., 2016. Migrating glioma cells express stem cell markers and give rise to new tumors upon xenografting. J. Neurooncol. 130, 53–62. https://doi.org/10.1007/s11060-016-2221-y.
- Neves, A.R., Queiroz, J.F., Lima, S.A.C., Reis, S., 2017. Apo E-functionalization of solid lipid nanoparticles enhances brain drug delivery: uptake mechanism and transport pathways. Bioconjug. Chem. 28, 995–1004. https://doi.org/10.1021/acs. bioconichem.6b00705.
- Oyewumi, M.O., Mumper, R.J., 2003. Influence of formulation parameters on gadolinium entrapment and tumor cell uptake using folate-coated nanoparticles. Int. J. Pharm. 251, 85–97. https://doi.org/10.1016/S0378-5173(02)00587-2.
- Patel, M.M., Patel, B.M., 2017. Crossing the blood-brain barrier: recent advances in drug delivery to the brain. CNS Drugs 31, 109–133. https://doi.org/10.1007/s40263-016-0405-9.
- Quirk, B.J., Brandal, G., Donlon, S., Vera, J.C., Mang, T.S., Foy, A.B., Lew, S.M., Girotti, A.W., Jogal, S., LaViolette, P.S., Connelly, J.M., Whelan, H.T., 2015. Photodynamic therapy (PDT) for malignant brain tumors—where do we stand? Photodiagnosis Photodyn. Ther. 12, 530–544. https://doi.org/10.1016/j.pdpdt.2015.04.009.
- Ryu, H.J., Mahapatra, S.S., Yadav, S.K., Cho, J.W., 2013. Synthesis of click-coupled graphene sheet with chitosan: effective exfoliation and enhanced properties of their nanocomposites. Eur. Polym. J. 49, 2627–2634. https://doi.org/10.1016/j.eurpolymj.2013.06.005.
- Saul, J.M., Annapragada, A., Natarajan, J.V., Bellamkonda, R.V., 2003. Controlled targeting of liposomal doxorubicin via the folate receptor in vitro. J. Control. Release 92, 49–67. https://doi.org/10.1016/S0168-3659(03)00295-5.
- Stone, R., Willi, T., Rosen, Y., Mefford, O.T., Alexis, F., 2011. Targeted magnetic hyperthermia. Ther. Deliv. 2, 815–838. https://doi.org/10.4155/tde.11.48.
- Sun, C., Ding, Y., Zhou, L., Shi, D., Sun, L., Webster, T.J., Shen, Y., 2017. Noninvasive nanoparticle strategies for brain tumor targeting. Nanomedicine 13, 2605–2621. https://doi.org/10.1016/j.nano.2017.07.009.
- Sundararajan, P., Wang, J., Rosen, L.A., Procopio, A., Rosenberg, K., 2018. Engineering polymeric Janus particles for drug delivery using microfluidic solvent dissolution approach. Chem. Eng. Sci. 178, 199–210. https://doi.org/10.1016/j.ces.2017.12. 013
- Thomas, E., Colombeau, L., Gries, M., Peterlini, T., Mathieu, C., Thomas, N., Boura, C., Frochot, C., Vanderesse, R., Lux, F., 2017. Ultrasmall AGuIX theranostic nanoparticles for vascular-targeted interstitial photodynamic therapy of glioblastoma. Int. J. Nanomed. 12, 7075–7088. https://doi.org/10.2147/IJN.S141559.
- Tu, F., Lee, D., 2014. Shape-changing and amphiphilicity-reversing Janus particles with pH-responsive surfactant properties. J. Am. Chem. Soc. 136, 9999–10006. https:// doi.org/10.1021/ja503189r.
- Xia, Q.S., Ding, H.M., Ma, Y.Q., 2017. Can dual-ligand targeting enhance cellular uptake of nanoparticles? Nanoscale 9, 8982–8989. https://doi.org/10.1039/C7NR01020F.
- Zhang, Y., Kohler, N., Zhang, M., 2002. Surface modification of superparamagnetic magnetite nanoparticles and their intracellular uptake. Biomaterials 23, 1553–1561. https://doi.org/10.1016/S0142-9612(01)00267-8.